

TITLE: Forecasting the Ring Current Index Dst in Real Time

AUTHORS: T. Paul O'Brien and Robert L. McPherron

AFFILIATION: Institute of Geophysics and Planetary Physics,  
405 Hilgard, UCLA, Los Angeles, CA 90095-1567

#### ABSTRACT

Three models for the evolution of the ring current index Dst are evaluated for real-time implementation. Each model provides the time evolution of Dst in terms of solar wind parameters. Real-time data resources employed by the models are Kyoto Quicklook Dst and ACE real-time solar wind parameters. The implementation described provides a forecast time of about 1 hour due to propagation of the solar wind from the ACE spacecraft to the Earth. The models are evaluated for simulated real-time data availability, and several error measures are provided. One-hour averages were used in keeping with the standard Dst index. By all measures used the model of O'Brien and McPherron (1999) performs best.

#### INTRODUCTION

When the interplanetary magnetic field (IMF) embedded in the solar wind opposes the Earth's intrinsic magnetic field, substantial transfer of energy into the terrestrial magnetosphere occurs. If this condition persists for several hours, the entire magnetosphere becomes disturbed—a situation termed a geomagnetic storm (Gonzalez et al., 1994). The primary measure of the intensity of a geomagnetic storm is the strength of the ring current, as measured by Dst. When hot ions are injected into the inner magnetosphere, the geometry of the geomagnetic field causes them to drift around the Earth forming a westward ring current. The magnetic field of the ring current decreases the field at the surface of the earth, and this depression is measured as Dst (Sugiura and Kamei, 1991; Mayaud 1980). A typical storm includes a substantial ring current that develops over a few hours and then recovers over several days (Kamide et al., 1997). Forecasting the state of the ring current is a necessity for forecasting the magnetic field in the magnetosphere (Baker, 1998). The Dst index represents the longest commonly used measure of the state of the ring current, and therefore it is essential in such forecasting. We will discuss the implementation and evaluation of three of the many models that forecast Dst in real-time.

In 1975 Burton et al. introduced a simple differential equation for the evolution of a corrected  $Dst^*$  in terms of solar wind conditions:

$$\frac{dDst^*}{dt} = Q(t) - \frac{Dst^*}{\tau} \quad (1)$$

The  $Q$  in this equation is proportional to the rate of energy injection into the ring current, and is generally given in terms of  $VB_s$ , the dawn-to-dusk component of the interplanetary electric field. Magnetic reconnection at the subsolar magnetopause is believed to allow part of the interplanetary electric field to enter the magnetosphere. In terms of the solar wind velocity and the interplanetary magnetic field (IMF) in Geocentric Solar Magnetospheric (GSM) coordinates,  $VB_s$  is defined as:

$$VB_s = \begin{cases} |VB_z| & B_z < 0 \\ 0 & B_z \geq 0 \end{cases} \quad (2)$$

The decay time  $\tau$  is usually given a value from 3 to 20 hours. This decay is attributed to ring current particles being lost to the atmosphere through precipitation and charge exchange.  $Dst^*$  is a corrected version of  $Dst$  with the contamination from magnetopause currents removed. The correction generally has the following form:

$$Dst^* = Dst - b\sqrt{P_{dyn}} + c \quad (3)$$

$P_{dyn}$  is the solar wind dynamic pressure, the force exerted on the magnetosphere by the flowing solar wind (Burton et al., 1975). An additional correction must be made for the effects of currents induced in the Earth, if one wants to estimate the energy in the ring current. We do not need to include this correction because it does not alter the dynamic equations or the pressure corrections determined from the standard  $Dst$ . Therefore, the quantity  $Dst^*$  is presumed to be proportional to the actual field perturbation caused by the ring current, but the effect of currents induced in the Earth is not removed. Hereafter, we will use the values of the parameters  $Q$ ,  $\tau$ ,  $b$ , and  $c$  to distinguish between three models of the evolution of the  $Dst$  index.

## OPERATIONAL CONSIDERATIONS

In order to turn a model of the above form into a real-time forecast, one must have an initial  $Dst$  and upstream solar wind measurements thereafter. The initial  $Dst$  is obtained from the Kyoto World Data

Center Quicklook Dst (<http://swdcd.db.kugi.kyoto-u.ac.jp/dstdir/dst1/q/Dstqthism.html>). This index is available every 12 hours typically, and may be delayed as much as 24 hours. The upstream solar wind measurements are obtained at the L1 point by the ACE spacecraft, and are made available in real time at the Space Environment Center (SEC) ([http://sec.noaa.gov/ace/ACERTsw\\_home.html](http://sec.noaa.gov/ace/ACERTsw_home.html)). The solar wind data are downloaded from SEC in real time, and propagated ballistically to the Earth. The propagation time from L1 to Earth is typically 1 hour, which is the reason we have a forecast rather than a nowcast. Once the solar wind data is propagated to the Earth, 1-hour averages are calculated for the velocity, number density, and magnetic field components in GSM. We have performed the 1-hour averaging to maintain consistency with the OMNI data set for which the models have been optimized. From these 1-hour averages, we calculate VBs and  $P_{dyn}$ . We are then able to use a simple forward-difference to integrate the Dst index from the Quicklook value to a 1-hour forecast:

$$Dst^*(t + \Delta t) = Dst^*(t) + \left[ Q(t) - \frac{Dst^*(t)}{t} \right] \Delta t \quad (4)$$

Conversions between  $Dst^*$  and Dst are performed according to Equation (3). We have simulated the real-time operation of this system for 3 different models of Dst, and we include below their performance.

### THREE MODELS

The first model we tried (AK1) has  $\tau$ ,  $b$ , and  $c$  as constants, and  $Q$  is a function of VBs. It is essentially the form of the original model proposed by Burton et al. (1975), but we have determined new coefficients based on the OMNI data set from 1964 to 1996, see Table 1. We solved the simultaneous least-squared-error equations to determine the optimal coefficients. The original Burton et al. work used 2.5-minute resolution data from 1967 and 1968 but determined the model coefficients by isolating periods when different processes were expected to dominate the Dst dynamics. The coefficients from the original Burton et al. work cannot be used because they did not use the standard algorithm for accommodating the magnetic latitude of the stations used in the calculation of Dst. The AK1 coefficients, however, are derived from the standard Dst, and do not suffer from this problem. The second model (UCB) is that of Fenrich and Luhmann (1998), which has  $b$  and  $c$  as constants, but  $\tau$  depends on VBs, and  $Q$  is a function of both  $P_{dyn}$  and VBs. The addition of the dynamic pressure  $P_{dyn}$  to the injection function is based on the assumption

that a stronger dynamic pressure facilitates more energy transfer to the magnetosphere through enhanced magnetic reconnection. The third model (AK2) is that of O'Brien and McPherron (1999), which has  $b$  and  $c$  as constants, but  $\tau$  and  $Q$  depend on VBs. The dependence of  $\tau$  on VBs is somewhat unusual. The authors hypothesize that during enhanced VBs the convection electric field in the magnetosphere is enhanced, moving the boundary between open and closed drift orbits—the presumed outer boundary of the symmetric ring current—to lower altitudes. At lower altitudes the denser exosphere provides more rapid charge exchange interactions, resulting in a more rapid decay of the ring current. For the reader's ease, the AK designation is an internal nomenclature referring to ACE-Kyoto, and the UCB designation refers to University of California Berkeley. These three models are given in detail in Table 1. It should be noted that each model is a single-step, first-order differential equation that provides the evolution of Dst entirely in terms of interplanetary conditions. Some further explanation of these models follows.

With respect to injection, the UCB  $Q$  equation is the most sophisticated, and includes a dynamic pressure contribution to energy transfer from the solar wind to the magnetosphere. The AK1 and AK2 models are more primitive, relying exclusively on the solar wind electric field to provide energy to the magnetosphere. In the AK1 model, the small offset of 0.5 mV/m does not seem to cause a substantial difference in predicted Dst, but introduces a catastrophic discontinuity in the simultaneous least-squares equations. Therefore, the cutoff of 0.5 mV/m has been removed to facilitate a simultaneous determination of all of the model coefficients. The cutoff value in AK2 was determined as part of  $Q$ , which was determined independently from the recovery and pressure correction terms. The UCB cutoff value was inherited from Burton et al., who also determined  $Q$  separately from the rest of the model. We now move to how the models handle ring current decay.

Of the equations for decay time, the AK2  $\tau$  equation is most sophisticated; it smoothly varies  $\tau$  from about 18 hours for zero VBs and 3 hours for very large VBs. The AK1 model makes no attempt at accommodating this variation, and relies exclusively on the value for zero VBs. The UCB model includes a piecewise decay by using a 3-hour decay time for large VBs, but uses a 7.7 hour decay time for weak to moderate VBs. The general impression one gets from the Fenrich and Luhmann (1998) paper and the O'Brien and McPherron (1999) paper is that the former concentrated on improving the equation for  $Q$ , while the latter focused on the equation for  $\tau$ . One might reasonably expect that the UCB model would

perform well during the main phase of a storm and the AK2 model would perform well during the recovery phase. The present results, however, do not conclusively support this supposition.

Another method of modeling the evolution of Dst is provided by Vassiliadis et al. (1999), who use 10-minute average data to fit parameters to a state-dependent second-order differential equation. They find that the parameters of the ring current model appear to depend on phase of the storm ( $dDst/dt$ ), Dst, and the input VBs, in such a way that the ring current model switches between first order and second order behavior at different times in the storm. They also find a wider range of recovery times between 25 and 2.5 hours, but these are not commensurate with the simple relation found by O'Brien and McPherron (1999). This more complex model is not included in our study because, at time of writing, it has not been implemented in real-time.

## ERROR EVALUATION

In order to estimate each model's operational performance, we simulated real-time data availability conditions. The simulation period was May 14 through December 31, 1998. We assumed that the Kyoto Quicklook Dst would be available at the second most recent Noon or Midnight, thereby causing a Kyoto lag of 12 to 24 hours behind real-time. One might expect that the periodic updating of the initial conditions from Kyoto would introduce jumps in the modeled Dst traces. However, the exponentially decaying nature of the models causes these changes in initial conditions to have dropped to the level of background by the time the intervening 12-hours have been integrated to reach real-time. We used the actual real-time ACE data, which we had archived locally, for the simulation period. About 10% of the period was covered by solar wind data gaps of 1-hour or more. We have included the ACE data gaps in our simulations to demonstrate the durability of the models to this very real operational problem. In Figure 1 we show the performance of all three models relative to the Kyoto provisional Dst for November 4 (day 308) through November 22 (day 326) of 1998. It is clear that the AK2 model best reproduces the variations in the Dst index. From day 320 onward, there is a large ACE data gap, and one can see that the three models decay smoothly to zero over different time scales. These are moderately intense disturbances, not necessarily representative of how these models perform on more severe disturbances. In general, it seems that the AK2 model Dst lies somewhere in between the UCB and AK1 values, with AK1 overshooting the

minimum Dst and UCB recovering too quickly. None of the three models accurately reproduces the minimum Dst on day 310. Summary error statistics are provided in Table 1. It should be noted that AK2 outperforms both of the other models in RMS error for the entire simulation and for those times when Dst was below -50 nT. Because recovery takes considerably longer than injection, most measurements of Dst < -50 nT correspond to recovery. Since the AK2 model outperforms the other two for Dst < -50 nT, which is dominated by recovery, we suggest that the  $\tau$  dependence on VBs is crucial in obtaining the correct recovery of the ring current. The larger errors for Dst below -50 nT are a reflection of both the difficulty in predicting large Dst and the uncertainty in the calculation of disturbed Dst.

The final error analysis we would like to show is the distribution of errors. Figure 2 shows the distribution, in 5 nT bins, of the errors made by each model. The UCB model seems to frequently provide a Dst value that is too high while the AK1 model seems to frequently provide a value that is too low. All three models have error distributions that are roughly Gaussian, but only AK2 is zero-centered. The Gaussian shape may be indicative of unpredictable randomness in the system. The fact that AK2 is zero-centered suggests that it may not accumulate large errors after many hours of evolution with solar wind data alone. Again, AK2 outperforms the other two models. The offset in the UCB model appears to be about 10 nT, almost exactly the difference between the  $c$  parameter in the UCB model and that of AK1 and AK2. However, even after adjusting  $c$  neither AK1 nor UCB would perform as well as AK2 in the Dst < -50 nT category.

## CONCLUSIONS

We have demonstrated an ability to provide somewhat reliable real-time Dst forecasts of about 1 hour. We have compared three models based on the ideas of Burton et al. (1975), and we have found that the AK2 model of O'Brien and McPherron (1999) outperforms the other two. This evaluation is based on a simulation of real-time data availability. The data needed for real-time implementation are Kyoto Quicklook Dst as an initial value and ACE real-time solar wind measurements from L1 for hourly evolution. The AK2 model seems to mitigate the overshoot and rapid recovery problems of the AK1 and UCB models. We believe that the better performance of the AK2 model results from its expression of the recovery time  $\tau$  in terms of the interplanetary electric field VBs.

## ACKNOWLEDGEMENTS

We would like to thank the Kyoto World Data Center for making the Quicklook and Provisional Dst available, the ACE spacecraft team and SEC for making the real-time solar wind data available, and the NSSDC for making the OMNI dataset available. We would like to acknowledge useful discussions with Janet Luhmann regarding the UCB real-time Dst model. This work was graciously supported by NSF grant NSF ATM 96-13667.

## REFERENCES

- Baker, D.N. (1998) What is space weather? *Advances in Space Research*, 22, pp. 7-16.
- Burton, R.K., R.L. McPherron, and C.T. Russell (1975) An empirical relationship between interplanetary conditions and Dst. *Journal of Geophysical Research* 80, pp. 4204-4214.
- Fenrich, F. R., and J. G. Luhmann (1998) Geomagnetic response to magnetic clouds of different polarity. *Geophysical Research Letters*, 25, pp. 2999-3002.
- Gonzalez, W.D., J.A. Joselyn, Y. Kamide, H.W. Kroehl, G. Rostoker, B.T. Tsurutani, and V.M. Vasyliunas (1994) What is a geomagnetic storm? *Journal of Geophysical Research*, 99, pp. 5771-5792.
- Kamide, Y., W. Baumjohann, I. Daglis, W.D. Gonzalez, M. Grande, J.A. Joselyn, R.L. McPherron, J.L. Phillips, G. Reeves, G. Rostoker, A.S. Sharma, H. Singer, B.S. Tsurutani, and V.M. Vasyliunas (1997) Current understanding of magnetic storms: Storm/substorm relationships. *Journal of Geophysical Research*, 103, pp. 17,705-17,728.
- Mayaud, P. N. (1980) *Derivation, Meaning and Use of Geomagnetic Indices*. Geophysical Monograph 22, AGU, Washington, D.C.,.
- O'Brien, T. P., and R. L. McPherron (1999) An Empirical Phase-Space Analysis of Ring Current Dynamics: Solar Wind Control of Injection and Decay. *Journal of Geophysical Research*, in press.
- Sugiura, M., and T. Kamei (1991) *Equatorial Dst index 1957-1986*, ISGI Publications Office.
- Vassiliadis, D., A. J. Klimas, and D. N. Baker (1999) Models of Dst geomagnetic activity and of its coupling to solar wind parameters, *Physics and Chemistry of the Earth*, 24, pp. 107-112.

Table 1. Comparison of the three real-time models.

Model	Q (nT/hour) (VBs in mV/m, P <sub>dyn</sub> in nPa)	τ (hours)	b (nT/√nPa)	c (nT)	RMSE (all Dst)	RMSE (Dst<-50nT)
AK1	$-2.47VB_s$	17.0	8.74	11.5	19 nT	38 nT
UCB (Fenrich and Luhmann, 1998)	$Q = \begin{cases} 0 & VB_s \leq 0.5 \\ -4.32(VB_s - 0.5)P_{dyn}^{1/3} & VB_s > 0.5 \end{cases}$	$\tau = \begin{cases} 7.7 & VB_s \leq 4 \\ 3 & VB_s > 4 \end{cases}$	15.8	20	21 nT	40 nT
AK2 (O'Brien and McPherron, 1999)	$-4.4(VB_s - 0.5)$	$24 \exp\left[\frac{9.74}{4.69 + VB_s}\right]$	7.26	11	16 nT	24 nT

Figure 1. Comparison of model Dst to Kyoto Dst for a disturbed period from November 4-22 (day 308-326) of 1998. Values were obtained using the real-time simulation described in the text.

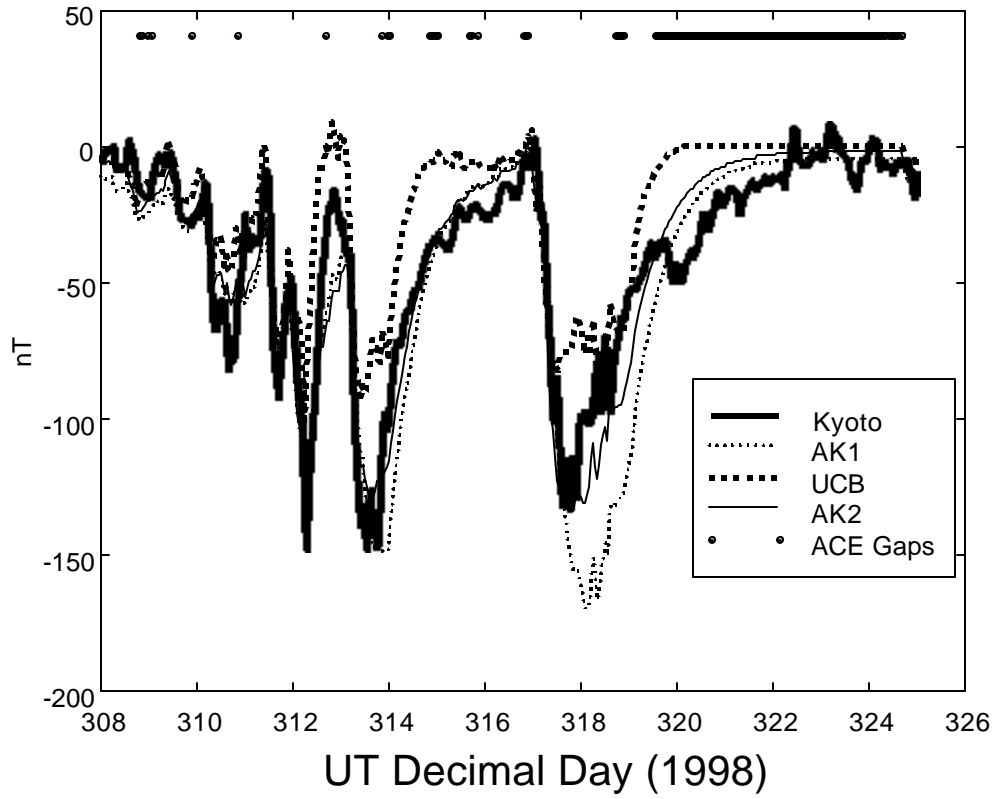


Figure 2. Distribution of hourly errors for each model. The bin size on the abscissa is 5 nT. Error is defined as Model-Dst.

